IEEE Access
Multidisciplinary | Rapid Review | Open Access Journal

Received February 11, 2018, accepted March 31, 2018, date of publication April 12, 2018, date of current version May 2, 2018.

Digital Object Identifier 10.1109/ACCESS.2018.2825255

Adaptive Coded Modulation Based on Continuous Phase Modulation for Inter-Satellite Links of Global Navigation Satellite Systems

RUI XUE[1], HUAN YU[1], AND QINGLIN CHENG[2]
[1]College of Information & Communication Engineering, Harbin Engineering University, Harbin 150001, China
[2]Shanghai Aerospace Electronic Technology Institute, Shanghai 201109, China

Corresponding authors: Huan Yu (yuhuan170924@hotmail.com) and Qinglin Cheng (32179907@qq.com)

This work was supported in part by the Shanghai Aerospace Science and Technology Innovation Fund under Grant SAST207-111, in part by the National Natural Science Foundation of China under Grant 61403093, in part by the National Defense Advance Research Program of Science and Technology under Grant 0104041, in part by the Open Research Fund of the State Key Laboratory of Space-Ground Integrated Information Technology under Grant 2015_SGIIT_KFJJ-DH_03, and in part by the Fundamental Research Funds for the Central Universities under Grant HEUCFP201769.

ABSTRACT The inter-satellite links (ISLs) will play an increasingly important role in improving the service performance and enhancing the survivability of global navigation satellite systems. The current signal transmission schemes in ISLs primarily employ constant coded modulation to guarantee a high reliable communication even for the worst channel status, and the adaptive coded modulation (ACM) schemes, such as binary low-density parity-check (LDPC) coded quadrature phase shift keying or M-ary quadrature amplitude modulation (MQAM) have been introduced to improve spectral efficiency over inter-satellite channels recently. However, the phase discontinuity of the above modulations will widen frequency spectrum and cause the high-voltage transient of transmitter, and the MQAM signal through high power amplifier onboard will result in non-linear distortion because of non-constant envelope. In this paper, the association between non-binary LDPC codes and high-order partial response continuous phase modulation with iterative detection is presented as the source of ACM schemes, which effectively inhibits information loss in the process of conversion between bit and symbol probabilities. According to the constellation of BeiDou navigation satellite system in 2020, an open loop ACM control mechanism based on inter-satellite distance is introduced, and implemented by the target bit error rate (BER) and the maximum ratio between the throughput and bandwidth algorithms. Simulation results show that the proposed ACM scheme can reduce the BER and improve the power efficiency in the requirement of target BER limit, and provide a higher spectral efficiency under the same transmitting power compared with the existing ACM scheme.

INDEX TERMS ACM, ISLs, CPM, LDPC, GNSS.

I. INTRODUCTION

Inter-satellite links (ISLs), also known as crosslinks, will be a promising technology to improve the reliability and integrity for global navigation satellite systems (GNSSs) [1]. By relying on the ISLs, a satellite navigation system can realize autonomous navigation, which means less dependence on ground facilities [2]. Under the support of ground infrastructures, orbit determination accuracy is substantially enhanced by combining ISLs and ranging observations from ground infrastructures. In addition, the interchange network composed of satellite-ground links and ISLs can also reduce the complexity and cut down operating cost in ground segment of GNSS. Although BeiDou navigation satellite system (BDS) has achieved considerable progress, it is still facing some difficulties and challenges due to a limited number of satellites, the current shortage of facilities and poor geometric distribution [3]. Introducing ISLs is a novel method to improve service quality and performance, therefore the next generation BDS will be a new system of navigation signal and ISLs.

ISL as a 'bridge' between two space vehicles is applied to transmit various information including system data, ranging

data, clock errors and so on. Its main function is inter-satellite ranging and communication [4]. At present, GNSSs are generally equipped with two kinds of channels that are the low rate omnidirectional telemetry, tracking, & Command (TT&C) channel and high rate data service channel by which to realize the functions measurement & control and data transmission separately. However, TT&C system and communication system are mutually independent, and the repeated construction is evidently harmful to economic benefits. Moreover, business users have different requirements for TT&C datum, and coordination work is quite complicated. The above two channels integration is an effective means to simplify the equipment onboard, improve the electromagnetic compatibility, reduce power consumption and save frequency resources, and the core issue in the combination is to design an integrated signal model with dual functions of ranging and communication. It is speculated that ISLs in the future GNSSs will be an integration of ranging and communication and thereby realize autonomous navigation [5].

The compound of ranging and communication is not a simple function overlay but a deep fusion, which primarily involves the design of channel coding, modulation, ranging code, carrier frequency and so on, and modulation scheme is one of the research emphasis. Continuous phase modulation (CPM) [6] has aroused extensive attention from scholars at home and abroad due to the characteristics of constant envelope and continuous phase, which can effectively inhibit nonlinear distortions and obtain high spectral efficiency with compact power spectral density (PSD) [7], [8]. CPM has been widely used in many systems by now, such as satellite communications [9], [10], satellite mesh networks [11], [12], digital video broadcasting (DVB) [13], [14], fiber-optical communications [15], telemetry [16], [17], and so on. In addition, our previous research results have indicated that certain CPM solutions can not only meet the compatibility requirement in the band S or C and reduce the complexity of user terminal, but also provide a better performance in the aspects of tracking precision, multi-path mitigation and anti-jamming compared to other modulation candidates [18], [19]. Consequently, it is feasible to design an integrated signal model of communication and ranging based on the CPM signals.

The distance between two satellites is changing with the relative motion, and power attenuation may vary greatly with inter-satellite distance. The maximum deviation of power loss is up to 20 dB. To ensure the reliability of signal transmission at the farthest distance, ISLs usually adopt a constant coded modulation (CCM) in the whole constellation to cope with the worst-case scenario, which inevitably results in system resource waste when the inter-satellite distance is getting shorter. For improving spectral efficiency over inter-satellite channels, [20] has employed the adaptive coded modulation (ACM) schemes i.e. binary low-density parity-check (LDPC) coded quadrature phase shift keying (QPSK) and M-ary quadrature amplitude modulation, and the throughput of the ACM scheme is nearly six times that of the CCM (QPSK and LDPC code rate 1/2). However, the phase discontinuity of legacy modulations will widen frequency spectrum and cause the high-voltage transient of transmitter, and the QAM signal through high power amplifier (HPA) onboard will cause non-linear distortion because of non-constant envelope. Besides, the scheme of binary LDPC coded high-order modulations would face with a difficult problem that is significant information loss in the process of conversion between bit and symbol probabilities [21]. In view of these problems in binary LDPC coded QPSK or MQAM, non-binary LDPC (NB-LDPC) codes combined with high-order partial response CPM (PRCPM) are introduced by this paper as the source of ACM schemes.

The rest of this paper is organized as follows. Section II mainly elaborates the relationship between the received signal-to-noise ratio (SNR) and inter-satellite distance. An ACM scheme based on q-ary LDPC coded PRCPM for ISL communication is proposed in Section III, including basic principle of CPM, system model of the proposed scheme, and CMS selection and switching algorithm. Simulation results are discussed in Section IV. Finally, we conclude the paper in Section V.

II. THE FUNCTIONAL RELATIONSHIP BETWEEN THE RECEIVED SNR AND INTER-SATELLITE DISTANCE

A. INTER-SATELLITE DISTANCE IN BDS

It was officially reported that China launched more than 23 satellites by the end of 2016, including 5 Geostationary Earth Orbit (GEO), 5 Inclined Geosynchronous Orbit (IGSO) and 9 Medium Earth Orbit (MEO) satellites. The whole China and most Asia-Pacific regions can enjoy navigation service with positioning accuracy of better than 10 meters, speed of 0.2 m/s and time of 50 ns [22]. The ultimate constellation consisted by 5 GEO satellites, 27 MEO satellites and 3 IGSO satellites will be accomplished by 2020 [23]–[25]. The GSO satellites are located at 58.75°E, 80°E, 110.5°E, 140°E and 160°E separately. The inclination of the MEO satellite relative to the equatorial plane is 55°. The three IGSO satellites will move at an inclination of 118°E with an inclination of 55° [26]. According to [27], the semi-major axis of GSO, IGSO and MEO are 42157.4 Km, 42157.4 Km and 27899.4 Km separately. In this paper, the final version of BDS with 35 satellites in the whole constellation is considered, as shown in Figure 1.

According to orbital altitude, ISLs can be classified into two groups: intra-layer ISLs with the same orbital altitude (MEO–MEO, GSO–IGSO) and inter-layer ISLs with different orbital altitude (IGSO–MEO, GSO–MEO), where the former can be divided into intra-plane ISLs and inter-plane ISLs [20]. More details about inter-satellite distance in the constellation are shown in Table 1. As we see from Table 1 that inter-satellite distance varies dramatically. The maximum value of inter-satellite distance is up to 68840.76 Km, and the minimum inter-satellite distance reaches up to 4567.50 Km.

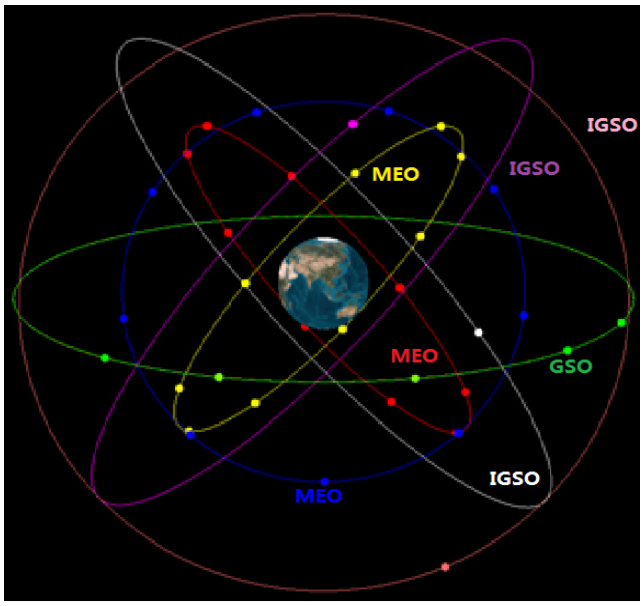

FIGURE 1. The final satellite constellation of BDS.

TABLE 1. Inter-satellite distance in the final constellation of BDS.

Type of ISL	Maximum Inter-satellite Distance, Km	Minimum Inter-satellite Distance, Km
MEO-MEO (INTRA-PLANE)	48323.47	19084.08
MEO-MEO (INTER-PLANE)	54327.36	5827.24
IGSO-MEO	68838.81	14258.01
GSO-MEO	68840.76	14258.00
GSO-IGSO	53698.92	4567.50

B. PROPAGATION LOSS IN FREE SPACE

Rain attenuation is seen as the dominant damage in the satellite-to-ground communication link because it gives rise to the maximum amount of loss [28]. Besides rain attenuation, transmitting time-delay and ranging error caused by the earth atmosphere under Ka would be relatively huge. By contrast, the major communication loss of satellite-to-satellite link is free space propagation loss which is largely dependent upon inter-satellite distance. According to [29], a formula is given for calculating the free space propagation loss, i.e.

$$L = \left(\frac{4\pi d}{\lambda}\right)^2 = \left(\frac{4\pi df}{c}\right)^2, \quad (1)$$

where the d is the inter-satellite distance, λ is the carrier wavelength, f is the carrier frequency, and c is the speed of light.

ISLs tend to use the same frequency band as satellite-to-ground links, and frequency band has been transited from ultra high frequency (UHF), L, S and C to Ka and V gradually because of huge communication capacity, strong anti-interference ability, fast transmission speed, and so on. The GPS III plans to increase Ka band ISLs and realize satellite-earth integration by combining ISLs with high speed uplink and downlink, which will be able to "contact one satellite, contact all satellites." [30]. So Ka band (30/20 GHz) is assumed to utilize in the ISLs of the future BDS.

As shown in Table 2, the free space propagation loss is getting bigger with the increasing of frequency at the same inter-satellite distance. It is noteworthy that the differential value of free space propagation loss between the maximum and minimum inter-satellite distance is more than 23 dB when the carrier frequency f is varied from 20 GHz to 30 GHz, which means link margin is relatively great at short inter-satellite distance. For a fixed coded modulation, there is a waste of spectrum resources. From this point of view, ACM technique is an effective ways to improve the spectral efficiency.

TABLE 2. The free space propagation loss of ISLs with distance.

Inter-satellite Distance, Km	Free Space propagation Loss, dB (f=20 GHz)	Free Space propagation Loss, dB (f=30 GHz)
68840.76 (Maximum)	215.22	218.75
4567.50 (Minimum)	191.65	195.18

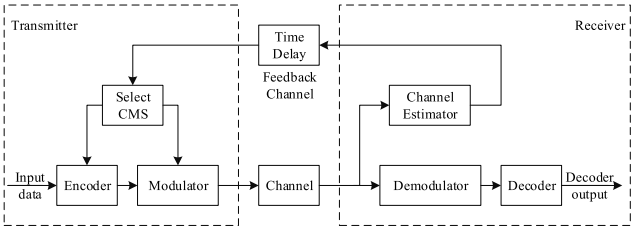

FIGURE 2. The principle block diagram of ACM.

C. SNR ESTIMATION BASED ON THE INTERSATELLITE DISTANCE

ACM is an important and efficient link adaptive transmission strategy, whose components are shown in Figure 2. The transmitter of ACM can flexibly adjust coded modulation scheme (CMS) including coding type, code length, code rate, modulation mode, modulation order, etc. according to channel status delivered by channel estimator in the receiver [31]. The transmission scheme dynamically match channel states for taking full advantage of the channel capacity while maintaining the same transmitted power. Note that the feedback channel is a bridge connecting the receiver and transmitter, and the control mechanism of ACM is a closed loop. The closed loop control mechanism seems surface to be unsuitable for ISLs in GNSSs. However, any satellite in the constellation usually stores the almanac of all satellites, and the location of each satellite at any moment can be calculated through the almanac. Once the position of two satellites is known, the inter-satellite distance between two satellites can be easily calculated. Since the transmission loss mainly originates from

the free space path loss, the SNR at the receiving terminal can be estimated according to the inter-satellite distance [20]. Each satellite can estimate the channel states individually using almanac of all the satellites, and the feedback channel is not necessary anymore. Through the above analysis, we can see that open loop control mechanism is feasible for ISLs.

The signal transmission loss on the ISLs is mainly made up of free space path loss, antenna pointing loss, polarization loss and so on, and free space path loss in the signal transmission loss counts for a dominant proportion. Based on the free space propagation formula provided by [29], the received signal power P_r is provided as follows:

$$P_r = \frac{P_t G_t G_r}{(4\pi d/\lambda)^2}, \tag{2}$$

where P_t is the emission signal power, G_t is the emitting antenna gain, G_r is the receiving antenna gain, d is the distance between two satellites, λ is the wavelength of carrier [20], and $P_t G_t$ is also denoted as effective isotropic radiated power (EIRP).

The receiving normalized SNR, i.e. E_b/N_0 can be expressed as

$$\frac{E_b}{N_0} = \frac{P_r}{N_0 R} = \frac{P_r}{KTR} = \frac{P_t G_t G_r}{(4\pi d/\lambda)^2 KTR}, \tag{3}$$

where E_b is the energy of one bit, N_0 is the noise PSD, R is the rate of information, K is the Boltzmann constant, T is the noise temperature of the receiver. Equation (3) can also be converted into a dB level version, and described as

$$\frac{E_b}{N_0} = \text{EIRP} + G_r - 20\lg(\frac{4\pi d}{\lambda}) - N_0 - R. \tag{4}$$

The receiving antenna gain G_r can be calculated by

$$G_r = (G/T) + T_r, \tag{5}$$

where G/T is the quality factor of the receiving antenna, T_r is the system noise. L_0 is defined as system margin and should be greater than other loss except path loss. According to [20], L_0 is set as 5 dB. The E_b/N_0 is rewritten as

$$\frac{E_b}{N_0} = \text{EIRP} + \frac{G}{T} + T_r - 20\lg(\frac{4\pi d}{\lambda}) - N_0 - R - L_0. \tag{6}$$

It must be pointed out that not all satellites in view could be ISL connected. The antenna pattern, radiation angle, transmitting power of satellite as well as modulation scheme are important factors for establishing ISLs. In this paper, we focus on the ACM scheme based on CPM applied to ISLs that have already been built up.

III. INTER-SATELLITE ACM COMMUNICATION SYSTEM

A. CONTINUOUS PHASE MODULATION (CPM)

Some attractive modulation options have emerged for ISLs communication, the prominent role is played by QPSK and MQAM. But phase discontinuity of the two modulations would widen frequency spectrum and cause the high-voltage transient of transmitter. Besides, the MQAM signal through high power amplifier (HPA) onboard will result in nonlinear distortion because of non-constant envelope. CPM is a class of constant envelope modulation that offers a relatively low spectral occupancy by introducing inter-symbol interference [32]. The characteristics of constant envelope and continuous phase make it very suitable for bandwidth-limited systems with nonlinear power amplifiers, for instance, satellite communication and satellite navigation. CPM is more than just a digital modulation, which is actually a combination of coding and modulation, i.e. a cascade of a time-invariant continuous phase encoder (CPE) and a time-invariant memoryless modulator (MM) [33].

Based on construction's feature of CPM, some researchers introduced a series of channel codes to connect with CPM for improving power efficiency. The concatenation of channel codes and CPM is commonly known as serially concatenated CPM (SCCPM). In order to improve BER performance and bandwidth efficiency, a few of forward error correcting (FEC) codes with excellent performance, such as turbo [34] and LDPC code [35], have been applied to CPM. However, binary channel coding concatenated high-order CPM would suffer from serious information loss in the mutual conversion of bit and symbol probabilities. Beyond that, convergence threshold of the concatenation is still higher than the Shannon limit. To solve this problem, we employ q-ary ($q \geq 2$) LDPC coding as the external code in this paper.

The expression of CPM signals in time-domain [6] is defined by

$$s(t, \boldsymbol{\alpha}) = \sqrt{\frac{2E_s}{T}} \cos\left(2\pi f_0 t + \varphi\left(t, \alpha\right) + \varphi_0\right), \quad t \geq 0, \tag{7}$$

where E_s is the energy per symbol, T is the symbol period, f_0 is the carrier frequency, φ_0 is the initial phase offset which can be set to zero for coherent transmitting, and $\varphi\left(t, \boldsymbol{\alpha}\right)$ is the information carrying phase denoted as

$$\varphi\left(t, \boldsymbol{\alpha}\right) = 2\pi h \sum_{i=0}^{\infty} \alpha_i q(t - iT), \tag{8}$$

where $\boldsymbol{\alpha}$ is the sequence of the M-ary symbols ($\alpha_i \in \{\pm 1, \pm 3, \cdots, \pm(M-1)\}$), h is the modulation index and can be denoted as $h = m/p$ (m and p are relatively prime positive integers), $q(t)$ is the integral of a positive normalized frequency pulse $g(t)$, and $g(t)$ is nonzero for L symbol periods, with a fully response for $L = 1$ and a partial response for $L > 1$. The $g(t)$ can be a form of rectangular (REC), raised cosine (RC), or Gaussian minimum shift keying (GMSK) pulse and so on. Through (8) we can observe that infinite CPM signals can be obtained by choosing different frequency pulses $g(t)$, symbol periods LT, modulation index h and modulation order M. For convenience, the raised cosine pulse of length L is notated as LRC. Similarly, GMSK pulse of length L is notated as LGMSK. Moreover, 4M2REC indicates a CPM signal with modulation order 4 and rectangular pulse of length $2T$.

Reference [33] defined the physical tilted phase as

$$\phi(\tau + nT, \mathbf{U}) = R_{2\pi}\left[\begin{array}{l} 2\pi h R_p\left[\sum_{i=0}^{n-L} U_i\right] + 4\pi h \\ \sum_{i=0}^{L-1} U_{n-i} q(\tau + iT) + W(\tau) \end{array}\right], \quad 0 \le \tau < T, \quad (9)$$

where $U_i = (\alpha_i + (M-1))/2$, $R_x[\bullet]$ is a modulo-x function and $W(\tau)$ is a data-independent function expressed as follows:

$$W(\tau) = \pi h(M-1)\tau/T - 2\pi h(M-1)\sum_{i=0}^{L-1} q(\tau + iT) + \pi h(L-1)(M-1), \quad 0 \le \tau < T. \quad (10)$$

Combining (7), (8), (9) and (10), the modulated CPM signals are obtained as follows:

$$s(t, \mathbf{U}) = \sqrt{\frac{2E_s}{T}} \cos\left(2\pi f_1 t + \phi(t, \mathbf{U}) + \varphi_0\right), \quad (11)$$

where offset carrier $f_1 = f_0 - h(M-1)/2T$. Through (9) we can observe that the modulated signal is entirely determined by the current symbol U_n, the $L-1$ previous data symbols $[U_{n-1}, \cdots, U_{n-L+1}]$, and the accumulated value of $V_n = R_p\left(\sum_{i=0}^{n-L} U_i\right)$. As shown in Figure 3, CPM can be decomposed into a continuous phase encoder and a memoryless modulator.

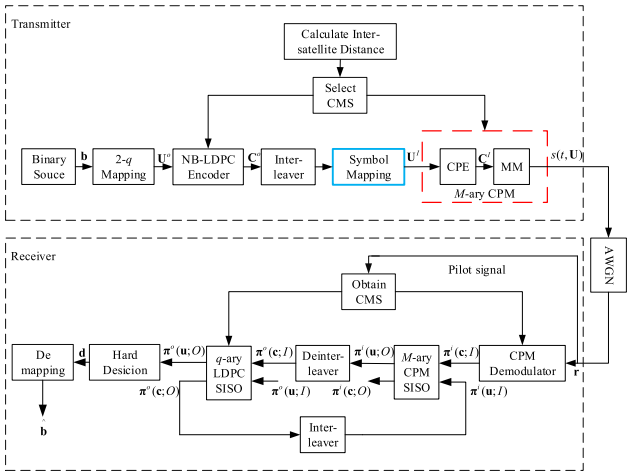

FIGURE 3. The transmission scheme of q-ary LDPC coded M-ary CPM as the source of ACM.

If M is assumed even, [36] has derived the autocorrelation function of CPM signals as follows:

$$\Re(\tau) = \frac{1}{T}\int_0^T \prod_{k=1-L}^{\lfloor \tau/T \rfloor} \times \frac{1}{M}\frac{\sin 2\pi h M\left[q(t+\tau-kT) - q(t-kT)\right]}{\sin 2\pi h\left[q(t+\tau-kT)\right]} dt, \quad (12)$$

where τ is the correlation time, and $\lfloor x \rfloor$ is the maximum integer below x. Based on the Wiener-Khintchine theorem, the PSD of CPM can be calculated by the Fourier transformation of $\Re(\tau)$, i.e.

$$\begin{aligned} P(f) = 2\Bigg\{ & \int_0^{LT} \Re(\tau)\cos 2\pi f\tau d\tau \\ & + \frac{1 - \psi(jh)\cos 2\pi fT}{1 + \psi^2(jh) - 2\psi(jh)\cos 2\pi fT} \\ & \cdot \int_{LT}^{(L+1)T} \Re(\tau)\cos 2\pi f\tau d\tau \\ & - \frac{\psi(jh)\sin 2\pi fT}{1 + \psi^2(jh) - 2\psi(jh)\cos 2\pi fT} \\ & \cdot \int_{LT}^{(L+1)T} \Re(\tau)\sin 2\pi f\tau d\tau \Bigg\} \end{aligned} \quad (13)$$

with $\psi(jh) = \sin M\pi h / M \sin \pi h$. From (13) we can see that the spectrum characteristics of CPM all depends on M, L, h and $g(t)$. As we know, the power of QPSK and MQAM within the first zero bandwidth makes up 90 percent of the total power. In order to maintain the effective power consistency, we can take advantage of (14) to calculate the bandwidth of CPM signals indirectly, i.e.

$$0.9 = \int_{-B_{90\%}/2}^{B_{90\%}/2} P(f) df. \quad (14)$$

B. STRUCTURE OF INTER-SATELLITE ACM COMMUNICATION SYSTEM

CPE can be considered as a convolutional code with a code rate of "1" due to the characteristics of memory and recursion. Figure 3 shows the transmission scheme of q-ary LDPC coded M-ary CPM over an additive white Gaussian noise (AWGN) with iterative decoding. The specific serially concatenated CPM can be established by combining q-ary LDPC code with CPE which can be viewed as an inner code. If code rate γ and codeword length Y of LDPC code have been given, a sparse parity check matrix $\mathbf{H} = [h_{i,j}]_{X \times Y}$ ($X = Y(1-\gamma)$) with $h_{i,j} \in \mathrm{GF}(q = 2^b)$ (b is a positive integer) is needed to provide. The generator matrix $\mathbf{G}$ can be obtained through Gaussian elimination if the $\mathbf{H}$ is a large-scale sparse matrix. At the transmitter, binary information sequence $\mathbf{b}$ is converted into information symbol sequence $\mathbf{U}^o = (U_0^o, U_1^o, \mathbf{L}, U_{k-1}^o)$ with length $K = Y - X$ by '2-q' mapper whose output is taken to q-ary LDPC encoder. The codeword $\mathbf{C}^o = (C_0^o, C_1^o, \mathbf{L}, C_{k-1}^o)$ is then sent to interleaver and symbol mapping (e.g. Gray mapping) which is not necessary if the finite field size of the NB-LDPC encoder is equal to the alphabet size of CPM. The output of symbol mapper $\mathbf{U}^i$ is delivered to M-ary continuous phase modulator, then the modulated sequence $s(t, \mathbf{U})$ is transmitted to an AWGN channel. For simplicity in the design, the module of symbol mapping can be eliminated as long as q is equal to M.

Compared to the traditional receiver, the most prominent feature of the investigated receiver is to adopt an iterative structure which mainly composes of two soft-input soft-output (SISO) decoders. The one decoder is for the inner CPE, the other is for the outer q-ary LDPC encoder.

The detection of demodulation and decoding is implemented by iteration described as 'outer iteration' between CPM-SISO and LDPC-SISO. The Log-MAP algorithm is adopted by the CPM-SISO. A log-domain belief propagation decoding algorithm based on fast Fourier transform simplified as Log-FFT-BP [37] is employed by the LDPC-SISO, where iteration in the decoding process is described as 'inner iteration'. In our simulation, inner iteration is carried out five times per outer iteration. The SISO module takes in a priori probabilities of both information and code symbols by two input ports, then exports a posterior probabilities (APPs) of both information and code symbols [38] through two output ports. Finally, the decision device selects the largest information symbol of APP in the last iteration.

As we know, GPS is the only navigation constellation in orbit to install the transceiver equipment onto ISLs from the beginning of Block IIR, and a preliminary ISL network has been established. Unfortunately, each satellite in the constellation only connects with few designated satellites. The fully connected network will be realized with the development of relevant techniques, the network communication performance depends on single ISL's performance. Thus we simply consider the communication scheme in point-to-point link in this paper.

The open loop control mechanism of the proposed ACM scheme can be carried out by several steps as follows:

(1) In the initial state, the whole satellites in the constellation are by default set to the most reliable coded modulation scheme (CMS) which only supports the lowest transmission efficiency rate regardless of the distance between two satellites.

(2) Over the initial state, the distance between two satellites can be calculated if the almanac is available for the sender and receiver, and CMS is flexibly updated on the basis of inter-satellite distance. To be specific, the function relation between channel state and candidates is established according to the inter-satellite distance, and the guiding principle of CMS selection is that a CMS with a higher spectral efficiency will be adopted when the distance is getting closer. More details about CMS selection are shown in the Section 3.3. If the almanac is not available or expired, the default CMS is recovered to use instead.

(3) The configuration information of the selected CMS will be delivered to the receiver by pilot signal, and the information data through corresponding coding and modulation is sent to receiver by the data signal.

(4) The receiver obtains the CMS used by the sender from the pilot signal [20].

(5) The data is recovered by the receiver using the information of CMS.

(6) Repeat steps (2)∼(5).

C. CMS SELECTION AND SWITCHING ALGORITHM

In the ACM system, an appropriate CMS should be picked up from scheme library according to the current channel status. From the analysis in the Section 2.3, we have realized that the transmission loss is approximately equal to the free space propagation loss. Meanwhile, SNR at the receiving end can be calculated by inter-satellite distance. Therefore, the switching strategy of different CMS can be formulated on the basis of inter-satellite distance, as shown in Figure 4, where d is the distance between two satellites and $d \in$ [Min, Max], Min denotes the minimum distance (4567.50 Km) between two satellites in the whole constellation, and Max denotes the maximum distance (68840.76 Km) between two satellites in the same constellation.

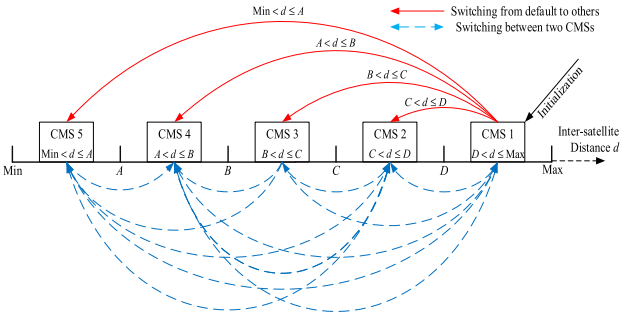

FIGURE 4. CMS switching strategy.

CMS 1∼CMS 5 are five alternative coded modulation schemes selected from the association of q-ary LDPC codes and M-ary PRCPM ($q = M \geq 2$) with different parameters of code rate, frequency pulse, modulation order and index etc., whose spectral efficiency is in ascending order. A, B, C and D are a series of threshold values which can be decided by different schemes switching algorithms, meeting the requirement for $A < B < C < D$. There are five intervals i.e. (min, A], (A, B], (B, C], (C, D], and (D, Max] to correspond to candidates from CMS 1 to CMS 5 respectively. CMS 1 is the default scheme after initialization, if the almanac on the satellite is available, the scheme updating from CMS 1 to others is implemented on the basis of inter-satellite distance d.

As a general rule, the binary channel coded high-order modulation scheme will suffer from serious information loss in the interconversion between bit probability and symbol probability. To address the problem, we employ the combination of q-ary LDPC codes and q-ary PRCPM to inhibit information loss as the result of using symbol probability directly rather than the interconversion of them. The CMS 1, CMS 2, CMS 3, CMS 4, and CMS 5 are five associations of q-ary LDPC coded PRCPM. The power and spectral efficiency is influenced by the parameters of coding and modulation mainly including code rate γ, frequency pulses $g(t)$, symbol periods LT, modulation index h and modulation order M. For example, a greater h will substantially improve the power efficiency at the cost of spectral efficiency while maintaining other parameters the same. Similarly, increasing M would improve the power efficiency and extend spectral occupancy at the same time. From (13) we can observe that increasing L or selecting a smooth $g(t)$ can effectively reduce

TABLE 3. Five CMSs in [20].

The reference CMS	FEC code	Code rate	Modulation	Modulation order	Spectrum efficiency, bit/s/Hz
1		1/2	QPSK	2	0.5
2	Binary	1/2	8QAM	3	0.75
3	LDPC	1/2	16QAM	4	1
4	Code	3/4	16QAM	4	1.5
5		5/6	64QAM	6	2.5

TABLE 4. The proposed five CMSs.

The proposed CMS	LDPC code	Code rate	Modulation	Modulation order	Modulation index	Spectrum efficiency, bit/s/Hz
1	Binary	3/4	2M2REC	1	4/5	0.83
2	4-ary	3/4	4M2RC	2	1/4	1.88
3	8-ary	3/4	8M2RC	3	1/8	2.74
4	8-ary	5/6	8M2REC	3	1/6	2.91
5	8-ary	3/4	8M2REC	3	1/10	4.33

the side lobe level, and enable most of the energy into the main lobe, which could lead to a rise in BER and reduces the power efficiency. A lower code rate will contribute to obtain the coding gain and result in a reduction in spectral efficiency at the same time. Besides the power and spectral efficiency, the implementation complexity of the whole system has to be considered and mainly primarily depends on CPM demodulator complexity which mainly lies on the number of matched filters. The modulation index h is a rational number of $h = m/p$ where m and p are relatively prime integers as described above, the complexity can be represented as pM^{L-1}. On the whole, these parameters should be designed comprehensively and give consideration to the power efficiency, spectral efficiency and implementation complexity.

An ACM scheme originated from several binary LDPC coded QPSK and MQAM is proposed by [20] for GNSS ISL's communication, as shown in Table 3. The five CMSs in Table 3 are regarded as the reference schemes in the course of parametric design process of q-ary LDPC coded PRCPM. In order to reduce the implementation complexity, this paper analyzes all CPM schemes subject to the constrain on $p \leq 10$, $L \leq 2$ and $M \leq 8$. In addition, different parameters of q-ary LDPC coded PRCPM schemes should provide superior performance in terms of power and spectral efficiency. Another five CMSs based on q-ary LDPC coded PRCPM are proposed to correspond to the five reference CMSs. More details are exhibited in Table 4.

The distance d between two satellites will determine a rational selection of CMS, and the CMS remains the same until the parameter d exceeds the setting threshold. In the meantime the state machine moves into a new state, and a different CMS is implemented. In this paper, two CMS switching algorithms named the target BER and maximum ratio between throughput and bandwidth (T/B) are introduced. Both of the adaptive algorithms are divided into four thresholds. The main difference of two algorithms is the derivation of threshold, and the specific value of the threshold has a strong influence on the ACM performance. Moreover, the threshold value can be flexibly adjusted according to the throughput of different user. The throughput is given by [20] as follows:

$$\text{Throughput} = R\,(1 - \text{FER}), \tag{15}$$

where R is the rate of the information and FER is the frame error rate.

In order to achieve high quality of service (QoS), the BER of some systems needs to be lower than the specific value which is called as the target BER. If more than one CMS meets the BER requirement, a CMS with the maximum spectral efficiency will be chosen. If the target BER has been given, the E_b/N_0 switching thresholds for coding and modulation can be acquired by simulation experiments. By contrast, the maximum T/B algorithm seeks the high transmission efficiency no limitation on BER. The details of the relationship between the inter-satellite distance and two CMS switching algorithms are exhibited in the Section IV.

IV. SIMULATION RESULTS AND ANALYSIS

The section mainly tests the validity of the proposed ACM scheme based on q-ary LDPC coded PRCPM applied in GNSS ISLs. Compared to the CMSs in [20] and the CCM (QPSK and LDPC code rate 1/2), the proposed scheme over an AWGN channel is evaluated by Monte Carlo simulations using MATLAB. In simulations, the inter-satellite distance in the constellation of BDS in 2020 with 35 satellites is considered. The carrier frequency is set to 30 GHz. EIRP and G/T are equal to 39 dBW and 2 dB/K separately. The binary information frame length is 600 bits, and the value of q is taken to 2, 4, and 8 respectively. In the q-ary LDPC encoder, it is assumed that q is always equal to M, which would mean the module of symbol mapper in Figure 3 is unnecessary. The $\mathbf{H}$ with lower triangular is derived byquasi-cyclic (QC) algorithm, and the $\mathbf{G}$ is obtained through Gaussian elimination [39], [40]. The q-ary LDPC codes employ

TABLE 5. Parameters of the two ACM scheme based on the target BER algorithm.

ACM schemes	Candidates	E_b/N_0, dB	Inter-satellite distance interval, Km
The proposed ACM	2*M*2REC-3/4	$E_b/N_0 < 5.77$	$d > D(53437.976)$
	4*M*2RC-3/4	$5.77 \le E_b/N_0 < 9.30$	$C(29060.628) < d \le D(53437.976)$
	8*M*2RC-3/4	$9.30 \le E_b/N_0 < 12.83$	$B(18362.212) < d \le C(29060.628)$
	8*M*2REC-5/6	$12.83 \le E_b/N_0 < 16.33$	$A(12936.149) < d \le B(18362.212)$
	8*M*2REC-3/4	$16.33 \le E_b/N_0$	$d \le A(12936.149)$
The reference ACM	QPSK-1/2	$E_b/N_0 < 6.23$	$d > D(50681.563)$
	8QAM-1/2	$6.23 \le E_b/N_0 < 10.90$	$C(25637.755) < d \le D(50681.563)$
	16QAM-1/2	$10.90 \le E_b/N_0 < 13.25$	$B(15971.106) < d \le C(25637.755)$
	16QAM-3/4	$13.25 \le E_b/N_0 < 16.62$	$A(8392.860) < d \le B(15971.106)$
	64QAM-5/6	$16.62 \le E_b/N_0$	$d \le A(8392.860)$

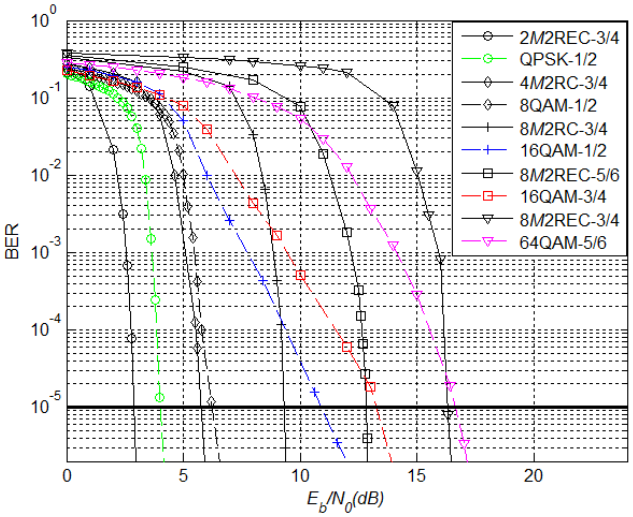

FIGURE 5. BER performance of the two ACM schemes.

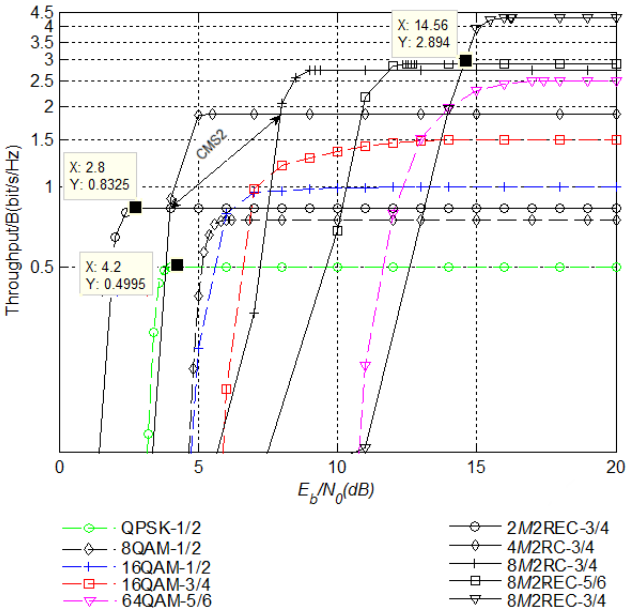

FIGURE 6. T/B performance of the two ACM schemes.

the Log-FFT-BP algorithm for decoding. The interleaves in the Figure 3 are all random interleavers. The CPM signals are decomposed into CPE and MM, and other parameters of CPM modulator are listed in Table 4. At last, the outer and inner iteration number are set to 8 and 5 respectively.

The target BER algorithm is fit for high QoS systems whose reliability should be guaranteed. In this paper, the target BER is set at 10^{-5}. The Figure 5 shows the BER performance versus E_b/N_0 for the proposed ACM scheme. We can observe from Figure 5 that all the alternatives based on CPM in the proposed ACM scheme could meet the requirement of BER limit when E_b/N_0 is in a certain region. In order to guarantee the uniqueness of scheme switching, the values of E_b/N_0 at BER $= 10^{-5}$ for different candidate do not coincide with each other. Each CMS in the proposed ACM scheme has a lower BER than the corresponding candidate in the reference scheme. For example, the E_b/N_0 value of the reference CMS 5' i.e. binary LDPC coded 64QAM with code rate 5/6 is 16.62 dB when BER is equal to 10^{-5}, and the proposed CMS 5 (8*M*2REC-3/4) just needs 16.33 dB at the same BER, which makes the latter have a gain of 0.29 dB. The gains of other proposed CMSs are larger than 0.29 dB and the maximum gain in the CMS 3 is approximately up to 1.60 dB. As a whole, the proposed ACM scheme shows a lower demand on E_b/N_0 than the reference one while achieving the target BER, which indicates the proposed ACM scheme can improve the power efficiency effectively under the same conditions. Finally, the inter-satellite distance interval for different CMS can be calculated by (6) if the switching region about E_b/N_0 is determined. More details about distance intervals are listed in Table 5.

The maximum T/B algorithm is proposed to maximize the total link throughput no restriction on the target BER. Although the transmission efficiency is effectively improved, the reliability could be getting worse. Thresholds for the

TABLE 6. Parameters of the two ACM scheme based on the maximum T/B algorithm.

ACM schemes	Candidates	E_b/N_0, dB	Inter-satellite distance interval, Km
The proposed ACM	2*M*2REC-3/4	$E_b/N_0 < 3.98$	$d > D(65667.427)$
	4*M*2RC-3/4	$3.98 \le E_b/N_0 < 7.95$	$C(33947.281) < d \le D(65667.427)$
	8*M*2RC-3/4	$7.95 \le E_b/N_0 < 11.87$	$B(20508.080) < d \le C(33947.281)$
	8*M*2REC-5/6	$11.87 \le E_b/N_0 < 14.56$	$A(15860.066) < d \le B(20508.080)$
	8*M*2REC-3/4	$14.56 \le E_b/N_0$	$d \le A(15860.066)$
The reference ACM	QPSK-1/2	$E_b/N_0 < 5.13$	$d > D(57524.122)$
	8QAM-1/2	$5.13 \le E_b/N_0 < 5.95$	$C(45329.403) < d \le D(57524.122)$
	16QAM-1/2	$5.95 \le E_b/N_0 < 6.99$	$B(32834.847) < d \le C(45329.403)$
	16QAM-3/4	$6.99 \le E_b/N_0 < 12.97$	$A(12776.444) < d \le B(32834.847)$
	64QAM-5/6	$12.97 \le E_b/N_0$	$d \le A(12776.444)$

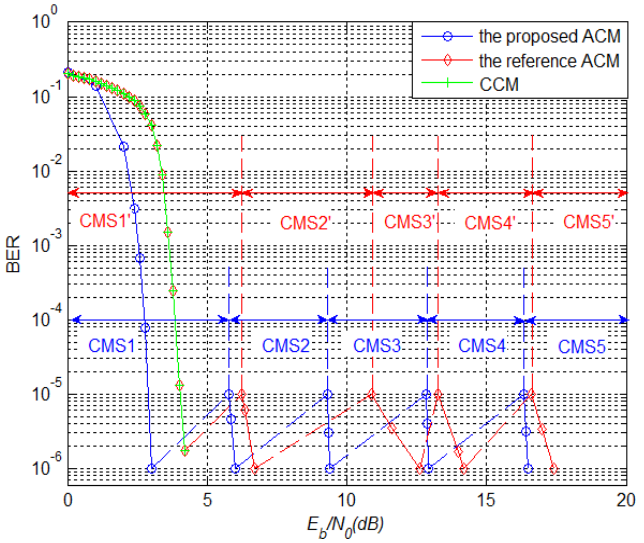

FIGURE 7. BER performance of the three schemes.

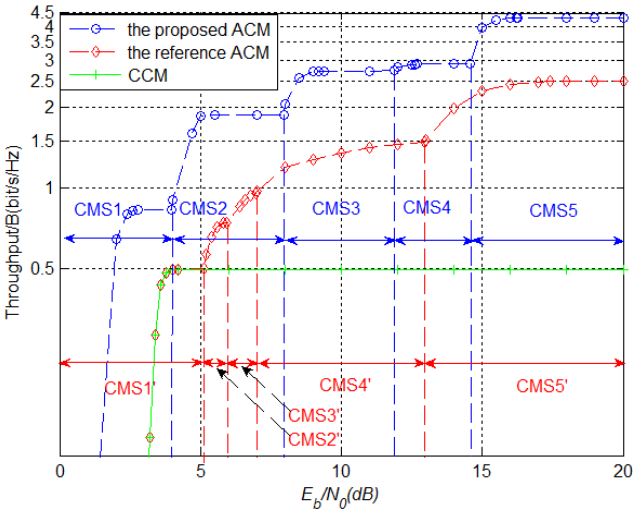

FIGURE 8. T/B performance of the three schemes.

parameter E_b/N_0 are those values for which the T/B curves related to different CMS are overlapped (Figure 6). The aim is to select, for each frame and E_b/N_0 value, the modulation order and the coding rate that maximize the total T/B. The final result is that the most efficient scheme in terms of T/B for E_b/N_0 value is selected [41]. As shown in Figure 6, the E_b/N_0 thresholds can be derived from the cross-points of CMS T/B curves. For instance, for values between 3.98 dB and 7.95 dB, the proposed CMS 2 (4*M*2RC-3/4) is the best choice because of the maximum T/B. If value exceeds the threshold limit, another CMS is put to use instead. When is greater than 14.56 dB, the CMS 5 (8*M*2REC-3/4) will be taken into account with the spectral efficiency 4.33 bit/s/Hz.

We also note from the Figure 6 that the maximum T/B of each CMS in the proposed ACM scheme is larger than the corresponding candidate in the reference scheme, and the former has a lower demand of E_b/N_0 at the same T/B than the latter. For instance, the proposed CMS 1 and the reference CMS 1' need 2.8 dB and 4.2 dB to reach the maximum T/B separately. We also note from the Figure 6, Table 3 and 4 that the spectral efficiency of CMS 1 is 1.66 times that of CMS 1', and the spectral efficiency gap between the two corresponding candidates is greater than 1.66 times. In other words, the proposed ACM scheme can significantly improve the spectral efficiency under the same transmitting power compared to the reference ACM scheme, which means the former is superior to the latter on the effectiveness of data delivering under the same circumstances. Likewise, the inter-satellite distance intervals corresponding to all CMSs can be calculated according to (6), as shown in Table 6.

Figure 7 shows BER curves versus E_b/N_0 for the three schemes including the proposed ACM, the reference scheme and CCM. It can be seen from Figure 7 that the reference ACM and CCM have the same BER performance when E_b/N_0 is in the range of 0∼4.2 dB, and the proposed ACM requires less E_b/N_0 to obtain the target BER limit than the reference ACM and CCM at the same region of E_b/N_0. We also observe from Table 5 and Figure 7 that each candidate in the proposed ACM scheme needs less E_b/N_0 value than

the corresponding candidate in the reference scheme to meet the requirements of target BER, which implies the proposed ACM scheme could save the transmitting signal power and improve the power efficiency at the same BER level compared to the reference one.

Figure 8 illustrates the T/B curves versus E_b/N_0 for the three schemes. It clearly appears that the reference ACM and CCM have the same T/B performance when E_b/N_0 is below 5.13 dB, over this threshold, the reference ACM has a better T/B performance than CCM. We also observe from Figure 8, Table 3 and Table 4 that the candidate in the proposed ACM scheme can obtain a higher spectral efficiency than the corresponding candidate in the reference scheme, the spectral efficiency gap of the corresponding alternative CMS between the two schemes is from 1.66 times to 2.74 times. Though the above analysis we deduce that the proposed ACM scheme can significantly improve the spectral efficiency under the same transmitting power compared to the reference ACM scheme.

V. CONCLUSION

The application of ACM technique for GNSS ISLs communication has been investigated in this paper. In the existing ACM solutions, the binary channel coded high-order modulation scheme would suffer from serious information loss in the interconversion between bit probability and symbol probability. Aiming at the issue, an ACM scheme with iterative detection and decoding based on q-ary LDPC coded PRCPM for ISL communication is proposed, where the adaptive processing mechanism is implemented by two algorithms, i.e. the target BER and the maximum T/B. The former is suitable for high QoS systems whose reliability should be guaranteed, and the latter pursues the high efficiency no limitation on BER. Simulation results over an AWGN channel based on MATLAB software show that compared to the reference ACM scheme, the proposed ACM can improve the power efficiency and reliability of information transmission, but also provide a higher spectral efficiency under the same transmitting power. Besides, every candidate in the proposed ACM scheme maintains the constant envelop and phase continuity characteristics of CPM, which enables the nonlinear power amplifier to operate near saturation and attains a low spectral occupancy property.

REFERENCES

[1] Y. Xie, "Relativistic time transfer for inter-satellite links," *Frontiers Astron. Space Sci.*, vol. 3, no. 15, pp. 1–6, Apr. 2016.

[2] H. Yan, Q. Zhang, Y. Sun, and J. Guo, "Contact plan design for navigation satellite network based on simulated annealing," in *Proc. IEEE Int. Conf. Commun. Softw. Netw.*, Chengdu, China, Jun. 2015, pp. 12–16.

[3] D. Yang, J. Yang, G. Li, Y. Zhou, and C. Tang, "Globalization highlight: Orbit determination using BeiDou inter-satellite ranging measurements," *GPS Solutions*, vol. 21, no. 3, pp. 1395–1404, Jul. 2017.

[4] J. Huang, Y. Su, L. Huang, W. Liu, and F. Wang, "An optimized snapshot division strategy for satellite network in GNSS," *IEEE Commun. Lett.*, vol. 20, no. 12, pp. 2406–2409, Dec. 2016.

[5] J. E. Valdez, B. Ashman, C. Gramling, G. W. Heckler, and R. Carpenter, "Navigation architecture for a space mobile network," in *Proc. Amer. Astron. Soc. Guid. Control Conf.*, Breckenridge, CO, USA, 2016, pp. 1–13.

[6] T. Aulin, N. Rydbeck, and C.-E. Sundberg, "Continuous phase modulation—Part II: Partial response signaling," *IEEE Trans. Commun.*, vol. COM-29, no. 3, pp. 210–225, Mar. 1981.

[7] L. Bing, T. Aulin, B. Bai, and H. Zhang, "Design and performance analysis of multiuser CPM with single user detection," *IEEE Trans. Wireless Commun.*, vol. 15, no. 6, pp. 4032–4044, Jun. 2016.

[8] X. Xie and Z. Xu, "Comparison of feedforward synchronization schemes for full-response CPM signals," *IEEE Access*, vol. 5, pp. 27376–27383, Dec. 2017.

[9] R. Xue, Y. Sun, and Q. Wei, "Dynamic iteration stopping algorithm for non-binary LDPC-coded high-order PRCPM in the Rayleigh fading channel," *EURASIP J. Wireless Commun. Netw.*, vol. 2016, no. 1, p. 62, Feb. 2016.

[10] Y. Yuan, B. Wang, and B. Wu, "Unified modulation and demodulation design for satellite communication systems," *Electron. Lett.*, vol. 52, no. 4, pp. 327–329, 2016.

[11] B. F. Beidas *et al.*, "Continuous phase modulation for broadband satellite communications: Design and trade-offs," *Int. J. Satellite Commun. Netw.*, vol. 31, no. 5, pp. 249–262, Mar. 2013.

[12] P. Remlein, "Energy efficient continuous phase modulation signals for satellite intelligent transportation systems," *IET Circuits, Devices Syst.*, vol. 8, no. 5, pp. 406–411, 2014.

[13] K. Ramadan, E. S. Hassan, X. Zhu, M. Abd-Elnaby, E. M. El-Sayed, and F. E. El-Samie, "Continuous phase modulation for digital video broadcasting," *Int. J. Comput. Appl.*, vol. 81, no. 1, pp. 45–52, Nov. 2013.

[14] K. A. Ramadan, E. S. M. El-Rabaie, M. A. EL-Nabi, E. S. Hassan, F. E. A. El-Samie, and X. Zhu, "Continuous phase modulation for digital video broadcasting and a chaotic interleaving with another OFDM version," *Programm. Device Circuits Syst.*, vol. 6, no. 8, pp. 223–232, Jan. 2014.

[15] T. F. Detwiler, S. M. Searcy, S. E. Ralph, and B. Basch, "Continuous phase modulation for fiber-optic links," *J. Lightw. Technol.*, vol. 29, no. 24, pp. 3659–3671, Dec. 15, 2011.

[16] J. Zhao, H. Liu, X. Chen, B. Zhang, and L. Zhao, "A new efficient key technology for space telemetry wireless data link: The low-complexity SC-CPM SC-FDE algorithm," in *Proc. Int. Conf. Inf. Commun. Technol.*, Nanjing, China, May 2014, pp. 4–10.

[17] D. Rieth, C. Heller, and G. Ascheid, "A novel modulation technique for spectral efficiency enhancement of ternary precoded continuous phase modulation," in *Proc. IEEE Int. Conf. Microw., Commun., Antennas Electron. Syst.*, Tel Aviv, Israel, Nov. 2015, pp. 1–5.

[18] R. Xue, Y. Sun, and D. Zhao, "CPM signals for satellite navigation in the S and C bands," *Sensors*, vol. 15, no. 6, pp. 13184–13200, Jun. 2015.

[19] R. Xue, Q.-M. Cao, and Q. Wei, "A flexible modulation scheme design for C-band GNSS signals," *Math. Problems Eng.*, vol. 2015, Jun. 2015, Art. no. 165097.

[20] J. Huang, Y. Su, W. Liu, and F. Wang, "Adaptive modulation and coding techniques for global navigation satellite system inter-satellite communication based on the channel condition," *IET Commun.*, vol. 10, no. 16, pp. 2091–2095, Oct. 2016.

[21] M. Zhu, Q. Guo, H. Xu, B. Bai, and X. Ma, "A multiple-voting-based decoding algorithm for nonbinary LDPC-coded modulation systems," *IEEE Access*, vol. 5, pp. 9739–9747, May 2017.

[22] S. Jin, "Preface: BeiDou navigation satellite system (BDS)/GNSS+: Recent progress and new applications," *Adv. Space Res.*, vol. 59, no. 3, pp. 751–752, Feb. 2017.

[23] C. Shi, Q. Zhao, Z. Hu, and J. Liu, "Precise relative positioning using real tracking data from COMPASS GEO and IGSO satellites," *GPS Solutions*, vol. 17, no. 1, pp. 103–119, Jan. 2013.

[24] X. Li, X. Zhang, X. Ren, M. Fritsche, J. Wickert, and H. Schuh, "Precise positioning with current multi-constellation global navigation satellite systems: GPS, GLONASS, Galileo and BeiDou," *Sci. Rep.*, vol. 5, Feb. 2015, Art. no. 8328.

[25] J. Guo, X. Xu, Q. Zhao, and J. Liu, "Precise orbit determination for quad-constellation satellites at Wuhan University: Strategy, result validation, and comparison," *J. Geodesy*, vol. 90, no. 2, pp. 143–159, Feb. 2016.

[26] Y. Sun, R. Xue, D. Wang, and D. Zhao, "Radio frequency compatibility evaluation of S band navigation signals for future BeiDou," *Sensors*, vol. 17, no. 5, pp. 1039–1058, May 2017.

[27] *BeiDou Navigation Satellite System Signal in Space Interface Control Document Open Service Signal*, China Satellite Navigat. Office, Beijing, China, 2016.

[28] J. X. Yeo, Y. H. Lee, and J. T. Ong, "Rain attenuation prediction model for satellite communications in tropical regions," *IEEE Trans. Antennas Propag.*, vol. 62, no. 11, pp. 5775–5781, Sep. 2014.
[29] M. Bousquet *et al.*, "Satellite communications and space telecommunications frequencies," in *Handbook of Satellite Applications*, J. N. Pelton, Ed. New York, NY, USA: Springer, 2013, Jan. 2015, pp. 239–270. [Online]. Available: http://www.springer.com/cn/book/9781441976710
[30] J. Clark, J. Langer, and T. Powell, "What GPS might have been—And what it could become," *Crosslinks*, vol. 11, pp. 70–77, Apr. 2010.
[31] A. J. Goldsmith and S.-G. Chua, "Adaptive coded modulation for fading channels," *IEEE Trans. Commun.*, vol. 46, no. 5, pp. 595–602, May 1998.
[32] C.-E. Sundberg, "Continuous phase modulation," *IEEE Commun. Mag.*, vol. CM-24, no. 4, pp. 25–38, Apr. 1986.
[33] B. E. Rimoldi, "A decomposition approach to CPM," *IEEE Trans. Inf. Theory*, vol. IT-34, no. 2, pp. 260–270, Mar. 1988.
[34] R. Xue, D.-F. Zhao, and T.-L. Zhu, "An improved method for the convergence of iterative detection in Turbo-CPM system," in *Proc. 5th Int. Conf. Wireless Commun. Netw. Mobile Comput.*, Beijing, China, 2009, pp. 1–5.
[35] X. Rui and X. Chun-li, "An improved iterative decoding method for LDPC coded CPM systems in Rayleigh fading channel," in *Proc. Int. Conf. Commun. Inf. Technol.*, Hammamet, Tunisia, 2012, pp. 341–346.
[36] J. B. Anderson *et al.*, *Digital Phase Modulation*. New York, NY, USA: Plenum, 1986, pp. 149–153. [Online]. Available: https://lib.ugent.be/catalog/rug01:001044891
[37] S. Hongzin and J. R. Cruz, "Reduced-complexity decoding of Q-ary LDPC codes for magnetic recording," *IEEE Trans. Magn.*, vol. 39, no. 2, pp. 1081–1087, Mar. 2003.
[38] S. Benedetto, D. Divsalar, G. Montorsi, and F. Pollara, "A soft-input soft-output APP module for iterative decoding of concatenated codes," *IEEE Commun. Lett.*, vol. 1, no. 1, pp. 22–24, Jan. 1997.
[39] J. Andrade *et al.*, "Design space exploration of LDPC decoders using high-level synthesis," *IEEE Access*, vol. 5, pp. 14600–14615, Jul. 2017.
[40] X.-Q. Jiang, H. Hai, H.-M. Wang, and M. H. Lee, "Constructing large girth QC protograph LDPC codes based on PSD-PEG algorithm," *IEEE Access*, vol. 5, pp. 13489–13500, Apr. 2017.
[41] R. Fantacci, D. Marabissi, D. Tarchi, and I. Habib, "Adaptive modulation and coding techniques for OFDMA systems," *IEEE Trans. Wireless Commun.*, vol. 8, no. 9, pp. 4876–4883, Sep. 2009.

RUI XUE received the M.S. and Ph.D. degrees in communication engineering and information & communication engineering from Harbin Engineering University, Harbin, China, in 2006 and 2009, respectively. Since 2003, he has been with the College of Information & Communication Engineering, Harbin Engineering University, where he is currently an Associate Professor. From 2011 to 2012, he was an Academic Visitor with the Nonlinear Signal Processing Laboratory, The University of Melbourne, Australia. . His research interests are in the area of radio mobile communication systems, satellite communication systems, and satellite navigation and positioning, and include error-correcting codes, high spectral efficiency modulation, coded modulation, iterative decoding and detection, and so on.

HUAN YU received the B.E. degree in communication engineering from Jilin University, Changchun, China, in 2016. She is currently pursuing the M.S. degree with the College of Information & Communication Engineering, Harbin Engineering University, Harbin, China. Her research interests include satellite communication and satellite navigation.

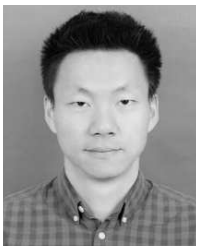

QINGLIN CHENG received the B.E. degree in communication engineering from Northwestern Polytechnical University, Xi'an, China, in 2010, and the M.S. degree in signal and information processing from the Shanghai Academy of Spaceflight Technology, Shanghai, China, in 2013. Since 2013, he has been with the Shanghai Academy of Spaceflight Technology. His research interests include software-defined radio and digital signal processing which are applied between space vehicles.